

# How to estimate time-varying Vector Autoregressive Models? A comparison of two methods.

Jonas Haslbeck  
Psychological Methods Group  
University of Amsterdam

Laura Bringmann  
University of Groningen

Lourens Waldorp  
Psychological Methods Group  
University of Amsterdam

June 17, 2022

## Abstract

The ubiquity of mobile devices led to a surge in intensive longitudinal (or time series) data of individuals. This is an exciting development because personalized models both naturally tackle the issue of heterogeneities between people and increase the validity of models for applications. A popular model for time series is the Vector Autoregressive (VAR) model, in which each variable is modeled as a linear function of all variables at previous time points. A key assumption of this model is that the parameters of the true data generating model are constant (or stationary) across time. The most straightforward way to check for time-varying parameters is to fit a model that allows for time-varying parameters. In the present paper we compare two methods to estimate time-varying VAR models: the first method uses a spline-approach to allow for time-varying parameters, the second uses kernel-smoothing. We report the performance of both methods and their stationary counterparts in an extensive simulation study that reflects the situations typically encountered in practice. We compare the performance of stationary and time-varying models and discuss the theoretical characteristics of all methods in the light of the simulation results. In addition, we provide a step-by-step tutorial for both methods showing how to estimate a time-varying VAR model on an openly available individual time series dataset.

## 1 Introduction

The ubiquity of mobile devices has led to a surge in intensive longitudinal (or time series) data sets from single individuals (e.g. Bringmann *et al.*, 2013; van der Krieke *et al.*, 2017; Kroeze *et al.*, 2016; Bak *et al.*, 2016; Hartmann *et al.*, 2015; Kramer *et al.*, 2014). This is an exciting development, because estimating models from data of single individuals naturally tackles the problem of differences between individuals. This is useful for psychological research, where heterogeneity between individuals

is a notorious problem. In addition, personalized models are potentially far more applicable in practice, since such models are tailored to the person at hand.

The key assumption when modeling time-series data is that all parameters of the true data generating model are constant (or stationary) across the measured time period. This is called the *assumption of stationarity*. While one often assumes constant parameters, changes of parameters over time are plausible in many situations: As an example, take the repeated measurements of the variables *Depressed Mood*, *Anxiety* and *Worrying*, modeled by a time-varying first-order Vector Autoregressive (VAR) model shown in Figure 1:

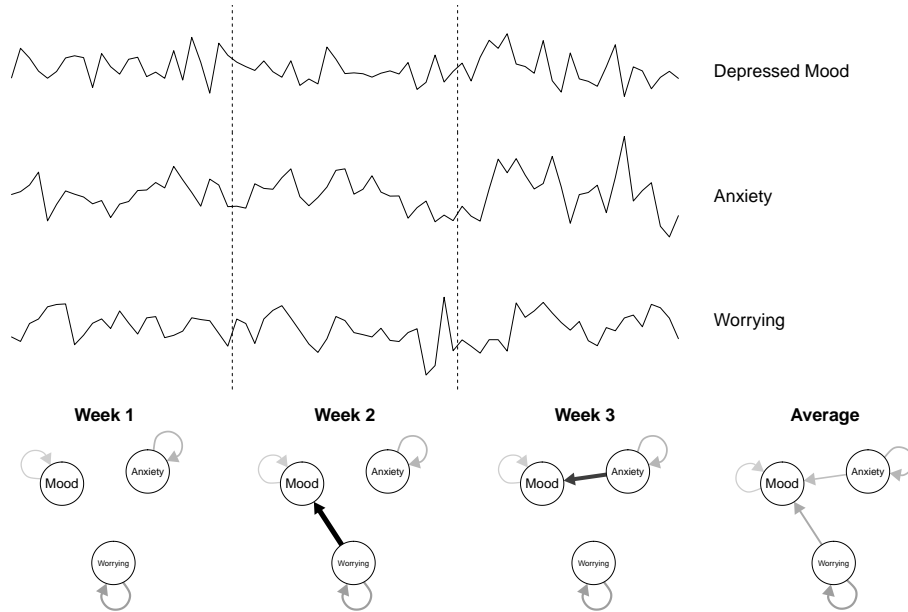


Figure 1: Upper panel: hypothetical repeated measurements of *Depressed Mood*, *Anxiety* and *Worrying*, generated from a time-varying lag 1 VAR model. Lower panel: the time-varying VAR-model generating the data shown in the upper panel. It consists of three models, one for each week. The fourth model (left to right) indicates the average of the three models, which is what one obtains when estimating a stationary VAR model on the entire time series.

In week 1, there are no cross-lagged effects between the three variables. However, in week 2 we observe a cross-lagged effect from *Worrying* on *Mood*. A possible explanation could be for instance a physical illness in week 2 that moderates the two cross-lagged effects. In week 3, we observe a cross-lagged effect from *Anxiety* on *Mood*. Again, this could be due to an unobserved moderator like a stressful period at work. The fourth visualization (from left to right) shows the average of the previous three models, which is the model one would obtain by estimating a stationary VAR model on the entire time series.

For these data, the stationary VAR model is clearly inappropriate, since it is an incorrect representation of *all* parts of the time series. In an applied context,

this means that we draw conclusions and design interventions based on an incorrect model. In addition, we miss the opportunity to identify unobserved moderator variables: for instance, if one finds a clear change in parameters at some point in the time series one could try to obtain additional data to explain this change (e.g. a critical event), or add variables that potentially explain it in future studies. Finally, continuously reestimating time-varying models on new data allows to *monitor* the changing dynamics in the VAR model, for instance during the period of an intervention.

The most straightforward way of dealing with non-stationary time-series data is to fit a non-stationary (or time-varying) model. In this paper we show how to estimate a time-varying version of the Vector Autoregressive (VAR) model, which is used in many of the papers cited above. The authors recently proposed different methods to estimate time-varying VAR models: Bringmann *et al.* (2015) presented an approach based on splines using the Generalized Additive Modeling (GAM) framework and Haslbeck and Waldorp (2015) suggested an approach based on penalized kernel-smoothing regression. While both methods are available to the applied researcher, it is unclear how well they perform in situations typically encountered in applied research. We improve this situation by making the following contributions:

1. We illustrate the performance of both methods in an extensive simulation study which reflects the type of time-series data typically encountered in practice
2. We discuss advantages and disadvantages of the characteristics of both methods in light of the simulation results
3. We compare time-varying methods to their corresponding stationary counterparts to address the question of how many observations are necessary to identify the time-varying nature of parameters
4. In two tutorials we give fully reproducible step-by-step descriptions of how to estimate time-varying VAR models using both methods on an openly available extensive longitudinal dataset

## 2 Estimating time-varying VAR models

In this section, we first introduce the notation for the stationary first-order VAR model and its time-varying extension (Section 2.1). We then present the two methods for estimating time-varying VAR models: the GAM based method (Section 2.2) and the penalized kernel-smoothing based method (Section 2.3). We discuss implementations of related methods in Section 2.4.

### 2.1 Vector Autoregressive (VAR) Model

In the Vector Autoregressive (VAR) model, the variables  $\mathbf{X}_t \in \mathbb{R}^p$  at time point  $t \in \mathbb{Z}$  are modeled as a linear combination of the same variables at earlier time points. If  $\mathbf{X}_t$  is only a function of the variables at the previous time point  $\mathbf{X}_{t-1}$ , we model  $\mathbf{X}_t$  as

$$\mathbf{X}_t = \boldsymbol{\beta}_0 + \mathbf{B}\mathbf{X}_{t-1} + \boldsymbol{\varepsilon} = \begin{bmatrix} X_{t,1} \\ \vdots \\ X_{t,p} \end{bmatrix} = \begin{bmatrix} \beta_{0,1} \\ \vdots \\ \beta_{0,p} \end{bmatrix} + \begin{bmatrix} \beta_{1,1} & \cdots & \beta_{1,p} \\ \vdots & \ddots & \vdots \\ \beta_{p,1} & \cdots & \beta_{p,p} \end{bmatrix} \begin{bmatrix} X_{t-1,1} \\ \vdots \\ X_{t-1,p} \end{bmatrix} + \begin{bmatrix} \epsilon_1 \\ \vdots \\ \epsilon_p \end{bmatrix}, \quad (1)$$

where  $\beta_{0,1}$  is the intercept of variable 1,  $\beta_{1,1}$  is the autoregressive effect of  $X_{t-1,1}$  on  $X_{t,1}$ , and  $\beta_{p,1}$  is the cross-lagged effect of  $X_{t-1,1}$  on  $X_{t,p}$ , and  $\boldsymbol{\varepsilon} = \{\epsilon_1, \dots, \epsilon_p\}$  are independent (across time points) samples drawn from a multivariate Gaussian distribution with variance-covariance matrix  $\Sigma$ . In this paper we do not model  $\Sigma$ . However, it can be obtained from the model and used to estimate the inverse covariance matrix (see e.g. Epskamp *et al.*, 2016).

Here and throughout the paper we deal with a first-order VAR model, in which all variables at time point  $t$  are a function of all variables at time point  $t - 1$ . In the interest of brevity we refer to this first-order VAR model (or VAR(1) model) as a VAR model. Additional lags can be added by appropriately augmenting the parameter matrix  $\mathbf{B}$  and the corresponding  $\mathbf{X}_{t-1}$  vector and the presented methods can be used to estimate VAR models with any set of lags. For a detailed description of VAR models we refer the reader to Hamilton (1994).

In both the GAM approach and the kernel-smoothing approach we estimate (1) by estimating each of the  $X_{t,i}$  for  $i \in \{1, \dots, p\}$  separately. Specifically, we model for all  $i \in \{1, \dots, p\}$

$$X_{t,i} = \beta_{0,i} + \boldsymbol{\beta}_i \mathbf{X}_{t-1} + \epsilon_i = \beta_{0,i} + [\beta_{i,1} \quad \cdots \quad \beta_{i,p}] \begin{bmatrix} X_{t-1,1} \\ \vdots \\ X_{t-1,p} \end{bmatrix} + \epsilon_i \quad (2)$$

where  $\boldsymbol{\beta}_i$  is the  $1 \times p$  vector containing the cross lagged effects on  $X_{t,i}$ . Then we combine the  $p$  models to the VAR(1) model in (1).

In order to turn the stationary VAR model in (1) into a time-varying VAR model, we introduce a time index for the parameter matrices  $\boldsymbol{\beta}_{0,t}$  and  $\mathbf{B}_t$ . This allows a different parameterization of the VAR model at *each time point* and hence lets the model vary across time. In the following two subsections we introduce two different ways to estimate such a time-varying VAR model.

## 2.2 The GAM Approach

In this approach, a time-varying VAR model is estimated by defining parameters as a spline function of time within the GAM framework (see also Bringmann *et al.*, 2017). GAM models are a non-parametric extension of General Linear Models in which linear predictors are substituted by non-parametric (smooth) functions (i.e.,  $\boldsymbol{\beta}_{0,t}$  and  $\mathbf{B}_t$ ). Here, the parameters are defined as a spline function of time, which allows us to obtain a time-varying model.

Since the spline function is twice continuously differentiable (smooth) everywhere, the key assumption of this method is that all true time-varying parameter functions are smooth as well. This assumption is also called the assumption of *local stationarity*, because smoothness implies that the parameter values at time points close to a given time point are very similar, and therefore locally stationary.

This assumption would for instance be violated by a step function. In this case the method would still correctly estimate the two constant parts, but will provide incorrect estimates around the ‘jump’ (e.g. as in Figure 4 (f) and (g)).

The GAM method proposed here is a penalized likelihood approach based on regression splines (Wood, 2006). In the time-varying VAR models inferred with this method, the time-varying parameters  $\beta_{0,t}$  and  $\beta_t$  are constructed from basis functions (see Figure 2). For instance, take a model with only an intercept, denoted  $\hat{\beta}_{0,t}$ . Such a model can be written as a sum of basis functions:

$$\hat{\beta}_{0,t} = \hat{\alpha}_1 R_1(t) + \hat{\alpha}_2 R_2(t) + \hat{\alpha}_3 R_3(t) + \dots + \hat{\alpha}_K R_K(t). \quad (3)$$

This equation consists of  $K$  known basis functions  $R_1(t), \dots, R_K(t)$  and  $K$  regression coefficients  $\hat{\alpha}_1, \dots, \hat{\alpha}_K$  that have to be estimated. In Figure 2 panel (b) through (f) one can see the five basis functions used for estimating a time-varying intercept  $\hat{\beta}_{0,t}$ , where the predictor time  $t$  is on the x axis. The final smooth function  $\hat{\beta}_{0,t}$  is obtained by adding up the weighted basis functions ( $\hat{\alpha}_K$ ) (see panel (g) and (h) of Figure 2). The optimal regression weights are estimated using standard linear regression techniques. The same rationale is applied to every time-varying parameter in the model.

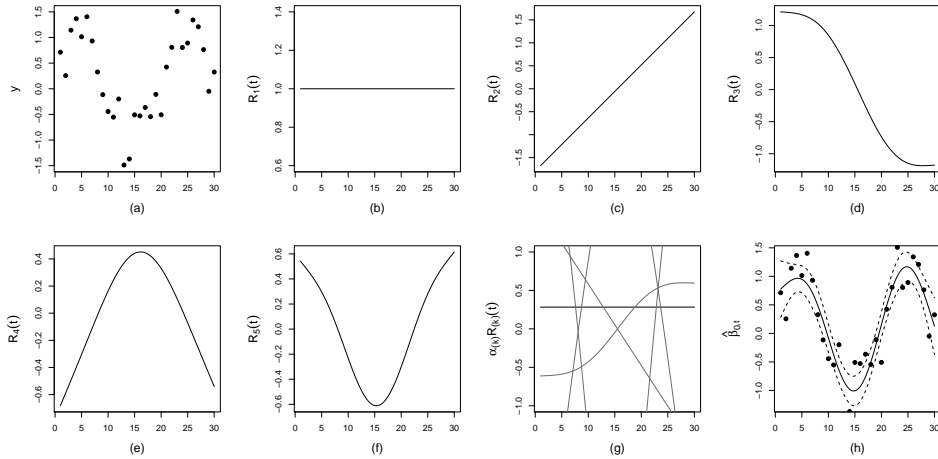


Figure 2: An example of the basis function for a time-varying parameter  $\hat{\beta}_{0,t}$ . In panel (a) the data are shown. In panel (b)-(f) the estimated 5 basis functions are given and panel (g) shows the weighted basis functions. In the last panel (h) the final smooth function is illustrated with credible intervals around the smooth function.

The regression spline basis used here is the thin plate regression spline basis (Wood, 2006). Thin plate regression splines, in contrast to standard regression splines such as cubic splines, are not knot-based in a conventional sense. This is because the basis functions are not directly related to a knot location (for more information see Wood, 2006). The mathematical forms of the first two basis functions ( $R_1$  and  $R_2$ ) are straightforward: one can recognize the constant and the first

predictor variable of a standard linear regression model. The other three basis functions ( $R_3 - R_5$ ) have a more complicated mathematical function (for examples, see Keele, 2008; Wood, 2006).

Fortunately, the choice of spline type is usually not crucial, as different spline bases tend to result in similar smooth functions (Wood, 2006). An example of the thin plate regression spline basis can be seen in Figure 2. The figure shows that each basis function brings the option of a higher complexity of the final smooth function. This is reflected in the fact that every extra basis function is more wiggly than the previous basis functions. For example, the last basis function in panel (f) is wigglier than the first basis function in panel (b). Note that all basis functions are gradual functions and thus cannot account for abrupt changes in the data.

The number of (regression spline) basis functions determines the complexity of the smooth function (e.g.,  $\hat{\beta}_{0,t}$ ). A key problem is how to choose the optimal number of basis functions: the final curve should be flexible enough to be able to recover the true model, but not too flexible to avoid overfitting (Andersen, 2009; Keele, 2008). The method used here to find the optimal number of basis functions is penalized likelihood estimation (Wood, 2006). Instead of trying to select the optimal number of basis functions directly, one can simply start by including more basis functions than would be normally expected, and then adjust for too much wiggleness with a *wiggleness penalty* (Wood, 2006). This means that what is now crucial is not the number of basis functions, but deciding on the right wiggleness penalty. This is done through generalized cross validation (Golub *et al.*, 1979). It is then the lowest Generalized Cross Validation (GCV) value that indicates the penalty with the best bias-variance trade-off. Penalization will decrease the influence of the basis functions ( $R$ ) by reducing the values of their regression coefficients ( $\hat{\alpha}$ ).

To estimate the GAM-based TV-VAR, we use the *tvvarGAM* package in *R* (Bringmann and Haslbeck, 2017). This is a wrapper around the *mgcv* package (Wood, 2006), to make it easier to estimate TV-VAR models with many variables. As the wiggleness penalty is automatically determined, the user only needs to specify a large enough number of basis functions. The default settings are the thin plate regression spline basis and 10 basis functions, which although an arbitrary number, is often sufficient (see the simulation results in Bringmann *et al.*, 2017). The minimum number is in most cases 3 basis functions. The GAM function in the *mgcv* package gives as output the final smooth function and the GCV value, as well as the effective degrees of freedom (edf) as a measure of nonlinearity. A linear function has an edf of one, and higher edf values indicate more wiggly smooth functions (Shadish *et al.*, 2014). Furthermore, the uncertainty of the smooth function is estimated with the 95% Bayesian credible intervals (Wood, 2006). In the remainder of this manuscript we refer to this method as the GAM method. A variant of the GAM method, in which we set parameters to zero whose 95% Bayesian credible interval overlaps with zero, we refer to as GAM(ts), for "significance thresholded". With GAM we refer to the standard unregularized VAR estimator.

After the model is estimated it is informative to check if the smooth functions were significant and if each smooth function had enough basis functions. Significance can be examined using the  $p$ -values of each specific smooth function, which tests if the smooth function is different from zero (over the whole time range). To see if there are enough basis functions, the edf of each smooth function can be examined, which should be well below the maximum possible edf or the number of basis functions

for the smooth function (or term) of interest (in our case 10, Wood, 2006). When the edf turns out to be too high, the model should be refitted with a larger (e.g., double) number of basis functions.

### 2.3 The Kernel-smoothing Approach

Similarly to the previous method, in the kernel-smoothing approach one estimates the  $p$  conditional distributions (2) separately, and then combine these to obtain the full VAR model (1). In the kernel-smoothing approach we obtain time-varying parameters by estimating several local models. Local models are estimated by weighting all observations depending on how close they are to the location of local model in the time series. In Figure 3 we show an example where a local model is estimated at time point  $t_e = 3$ . We do this by giving the time points close to  $t_e$  a high weight and time points far away from  $t_e$  a very small or zero weight. If we estimate models like this on a sequence of equally spaced estimation points across the whole time series and take all estimates together, we obtain a time-varying model.

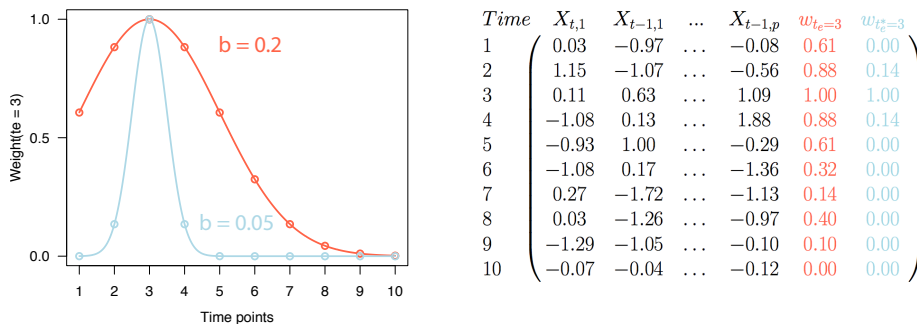


Figure 3: Illustration of the weights defined to estimate the model at time point  $t_e = 3$ . Left panel: a kernel function defines a weight for each time point in the time series. Right panel: the weights shown together with the VAR design matrix constructed to predict  $X_{t,1}$ .

Specifically, we use a Gaussian kernel  $\mathcal{N}(\mu = t_e, b^2)$  function to define a weight for each time point in the time series

$$w_{j,t_e} = \frac{1}{\sqrt{2\pi b^2}} \exp\left\{-\frac{(j - t_e)^2}{2b^2}\right\}, \quad (4)$$

where  $j \in \{1, 2, \dots, n\}$ .

It follows that the time point  $t_e = 3$  gets the highest weight, and the larger the distance of time points from  $t_e$  the smaller their weights becomes. The same idea is represented in the data matrix in the right panel of Figure 3: each time point in the multivariate time series is associated with a weight defined by the kernel function. The smaller we choose the bandwidth  $b$  of the kernel function, the smaller the number of observations we combine in order to estimate the model at  $t_e$ : when

using a kernel with bandwidth  $b = 0.2$  (red curve), we combine more observations than when using the kernel with  $b = 0.05$  (blue curve). The smaller the bandwidth the larger the sensitivity to detect changes in parameters over time. However, a small bandwidth means that less data is used and therefore the estimates are less reliable (only three time points, see right panel of Figure 3).

Since we combine observations close in time to be able to estimate a local model, we have to assume that the models close in time are also similar. This is equivalent to assuming that the true time-varying parameter functions are smooth, or locally stationary. Thus the key assumption of the kernel-smoothing approach is the same as in the spline approach.

The weights  $w_{j,t_e}$  defined in (4) enter the loss function of the  $\ell_1$ -regularized regression problem we use to estimate each of the  $p$  models in (2)

$$\hat{\beta}_{\mathbf{t}} = \arg_{\beta_{\mathbf{t}}} \min \left\{ \frac{1}{n} \sum_{j=1}^n w_{j,t_e} (X_{i,j} - \beta_{0,i,t} - \beta_{\mathbf{t}} \mathbf{X}_{t-1,j})^2 + \lambda_i \|\beta_{\mathbf{t}}\|_1 \right\}, \quad (5)$$

where  $X_{i,j}$  is the  $j$ th time point of the  $i$ th variable in the design matrix,  $\|\beta_{\mathbf{t}}\|_1 = \sum_{i=1}^p \sqrt{\beta_i^2}$  is the  $\ell_1$  norm of  $\beta_{\mathbf{t}}$ , and  $\lambda_i$  is a parameter controlling the strength of the penalty.

For each of the  $p$  regressions, we select the  $\lambda_i$  that minimizes the out of sample deviance in 10-fold cross validation (Friedman *et al.*, 2010). In order to select an appropriate bandwidth  $b$ , we choose the  $\hat{b}$  that minimizes the out of sample deviance *across* the  $p$  regressions in a time stratified cross validation scheme (for details see Haslbeck and Waldorp, 2015). We choose a constant bandwidth for all regressions so we have a constant bandwidth for estimating the whole VAR model. Otherwise the sensitivity to detect time-varying parameters and the trade-off between false positives and false negatives differs between parameters, which is undesirable.

In  $\ell_1$ -penalized (LASSO) regression the squared loss is minimized together with the  $\ell_1$ -norm of the parameter vector. This leads to a trade-off between fitting the data (minimizing squared loss) and keeping the size of the fitted parameters small (minimizing  $\ell_1$ -norm). Minimizing both together leads to small estimates being set to exactly zero, which is convenient for interpretation. When using  $\ell_1$ -penalized regression, we assume that the true model is sparse, which means that only a small number of parameters  $k$  in the true model are nonzero. If this assumption is violated, the largest true parameters will still be present, but small true parameters will be incorrectly set to zero. However, if we keep the number of parameters constant and let  $n \rightarrow \infty$ ,  $\ell_1$ -regularized regression also recovers the true model if the true model is not sparse. For an excellent treatment on  $\ell_1$ -regularized regression see Hastie *et al.* (2015).

As noted above, the larger the bandwidth  $b$ , the more data is used to estimate the model at a particular estimation point. Indeed, the data used for estimation is proportional to the area under the kernel function or the sum of the weights  $N_{\text{util}} = \sum_{j=1}^n w_{j,t_e}$ . Notice that  $N_{\text{util}}$  is smaller at the beginning and end of the time series than in the center, because the kernel function is truncated. This necessarily leads to a smaller sensitivity to detect effects at the beginning and the end of the time series. For a more detailed description of the kernel smoothing approach see also Haslbeck and Waldorp (2015). In the remainder of this manuscript we refer



to this method as KS(L1). With GLM(L1) we refer to the stationary  $\ell_1$  penalized estimator.

## 2.4 Related work

Several implementations of related models are available as free software packages. The R-package *earlywarnings* (Dakos and Lahti, 2013) implements the estimation of a time-varying AR model using a rolling window approach. The R-package *MARSS* (Holmes *et al.*, 2013, 2012) implements the estimation of (time-varying) state-space models, of which the time-varying VAR model is a special case. While the state-space model framework is very powerful due to its generality, it requires the user to specify the way parameters are allowed to vary over time, for which often no prior theory exists in practice (Belsley and Kuti, 1973; Tarvainen *et al.*, 2004). An interesting way to modeling time-varying parameters is by using the fused lasso (Hastie *et al.*, 2015). However, to our best knowledge there are currently only implementations available to estimate time-varying Gaussian Graphical Models with this type of method: a Python implementation (Monti, 2014) of the SINGLE algorithm (Monti *et al.*, 2014) and a Python implementation (Gibbert, 2017) of the (group) fused-lasso based method as presented in Gibberd and Nelson (2017).

## 3 Simulation A: Random graph

### 3.1 Data generation

We generated data from time-varying VAR models with  $p = 20$  variables and a sequence of time points  $n = \{20, 30, 36, 69, 103, 155, 234, 352, 530, 798, 1201, 1808\}$ , which are on log scale rounded to the nearest integer. We chose these values because they cover the large majority of scenarios applied researchers typically encounter. Importantly, in this setting increasing  $n$  does not mean that the time-interval gets longer, but it means that more observations are available in the same time-interval. For example, if the goal is to estimate the time-varying parameters of an individual in January, it is of no value to continue measuring in February. But the estimation problem becomes easier if we had more measurements in January.

We used the following procedure to specify whether a parameter is nonzero: we set all autocorrelations to be present and then randomly set 35 off-diagonal elements to be present, which corresponds to an edge-probability of  $P(\text{edge}) = 0.2$  rounded to the nearest integer. We set a fixed number of elements to nonzero instead of using draws with  $P(\text{edge}) = 0.2$ , because we resample the VAR matrix until it represents a stable VAR model (the absolute value of all eigenvalues is smaller than 1). By fixing the number of nonzero elements we avoid biasing  $P(\text{edge})$  through this resampling process. The rationale for setting all autocorrelations to be present is that this is both a reasonable assumption and an empirical finding in most applications (e.g. aan het Rot *et al.*, 2012; Snippe *et al.*, 2017; Wigman *et al.*, 2015). In addition, sampling autocorrelations with  $P(\text{edge})$  instead would lead to the unrealistic situation that almost all predictor pairs are uncorrelated. This approach gives us a  $p \times p$  matrix with 1s in the diagonal and zeros and 1s in the off-diagonal. If an edge (parameter) is defined to be present in this initial matrix, we assign with equal probability one of the parameter sequences (a) - (g) in Figure 4 to it.

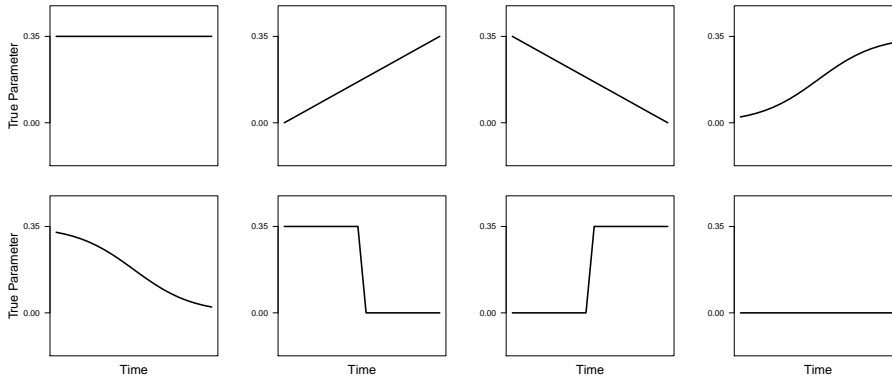


Figure 4: The eight types of time-varying parameters used in the simulation study: (a) constant nonzero, (b) linear increase, (c) linear decrease, (d) sigmoid increase, (e) sigmoid decrease, (f) step function up, (g) step function down, (h) constant zero.

If an edge is set to be absent in the initial graph, all entries of the edge weight sequence are set to zero (Figure 4 (h)). In each iteration we use this approach to generate a time-varying VAR for each of the  $n$  time points. This means that each time-varying VAR model is parameterized by a  $p \times p \times n$  array. We set the maximal parameter size of time-varying parameters to  $\theta = .35$  (see Figure 4) and we associated to each variable and time point a Gaussian noise process with variance  $\sigma^2 = \sqrt{0.1}$ . Hence the signal/noise ratio used in our setup is  $S/N = \frac{0.35}{0.1} = 3.5$ . All intercepts are set to zero and the covariances between the noise processes assigned to each variable is zero. We run 100 iterations of this design.

### 3.2 Estimation

We estimated the time-varying VAR model via KS(L1) method using the implementation in the R-package *mgm* (Haslbeck and Waldorp, 2015). In a first step we selected an appropriate bandwidth parameter by searching the candidate sequence  $\mathbf{b} = \{.01, .045, 0.08, 0.115, .185, .22, .225, .29, .325, .430, .465, 0.5\}$ . For  $n \leq 69$  we omit the first 5 values in  $\mathbf{b}$ , and for  $n > 69$  we omit the last 5 values. We did this to save computation time since for small  $n$  small  $b$  are never selected, and analogously for large  $n$  very large  $b$  values are never selected. To select an appropriate bandwidth parameter we use the following training set / test set scheme: we define a test set  $S_{\text{test}}$  by selecting  $|S_{\text{test}}| = \lceil (n * 0.2)^{2/3} \rceil$  time points stratified equally across the whole time series. We then estimate a time-varying VAR model for each variable  $p$  at each time point in  $S_{\text{test}}$  and predict the  $p$  values at that time point. We then compute for each  $b$  the  $|S_{\text{test}}| \times p$  absolute prediction errors and take the arithmetic mean. Then we select the bandwidth  $\hat{b}$  that minimizes this mean prediction error. Then for the fixed  $\hat{b}$ , we estimate the model on the full data using  $\hat{b}$  and  $\hat{\lambda}$  at 20 equally spaced time points, where we select an appropriate penalty parameter  $\hat{\lambda}_i$  with 10-fold cross-validation for each of the  $p$  variables.

In order to compare the  $\ell_1$ -regularized time-varying VAR estimator to a stationary  $\ell_1$ -regularized VAR estimator, we also estimate the latter using the *mgm* package.

The time-varying VAR model via the GAM method was estimated as implemented in the R-package *tvvarGAM* (Bringmann and Haslbeck, 2017). The tuning parameter of the spline method is the number of basis functions used in the spline regression. Previous simulations (Bringmann *et al.*, 2015) have shown that 10 basis functions give good estimates of time-varying parameters. To ensure that the model is identified, for a given number of basis functions  $k$  and variables  $p$ , we require *at least*  $n_{min} > (p + 1)k$  observations. In our simulation, we used this constraint to select the maximal number of basis functions possible given  $n$  and  $p$ , but we do not use less than 3 or more than 10 basis functions. Specifically, the selected number of basis functions  $k_s$  is defined as

$$k_s = \min \left\{ 3, \max \left\{ \max \left\{ k : k > \frac{(p+1)}{n} \right\}, 10 \right\} \right\}.$$

If  $k_s$  satisfies the above constraint, the time-varying VAR model can be estimated with the spline-based method. In the above setup the model is *not* the case for the cells  $n = \{20, 30, 46\}$ .

We also fit a standard stationary VAR model using linear regression to get the unbiased stationary counter-part of the GAM methods. The stationary VAR model is not identified for the cell  $n = 20$ , since the first row of the data matrix has to be omitted and hence  $p < n$ .

### 3.3 Results

In Section 3.3.1 we report the performance of the GLM, GLM(L1), KS(L1), GAM and GAM(st) methods in estimating different time-varying parameters *averaged across time*. The following Section 3.3.2 zooms in on the performance *across time*, for the constant and the linear increasing parameter function. In Section 3.3.3, we show the global performance in structure recovery of all methods. Finally, we report the computation time for the KS(L1) and GAM(st) methods in Section 3.3.4.

#### 3.3.1 Absolute error averaged over time

Figure 5 shows the absolute error, averaged over time-varying parameters of the same type (see Figure 4), time points and iterations as a function of the number of observations  $n$  on a log scale. On the y-axis we show the absolute estimation error, which can be interpreted as follows: let's say we are in the scenario with  $n = 155$  observations and estimate the constant function in Figure 5 (a) with the stationary  $\ell_1$ -regularized regression GLM(L1). Then the *expected* average (across the time series) absolute error of the constant function is  $\pm 0.09$ .

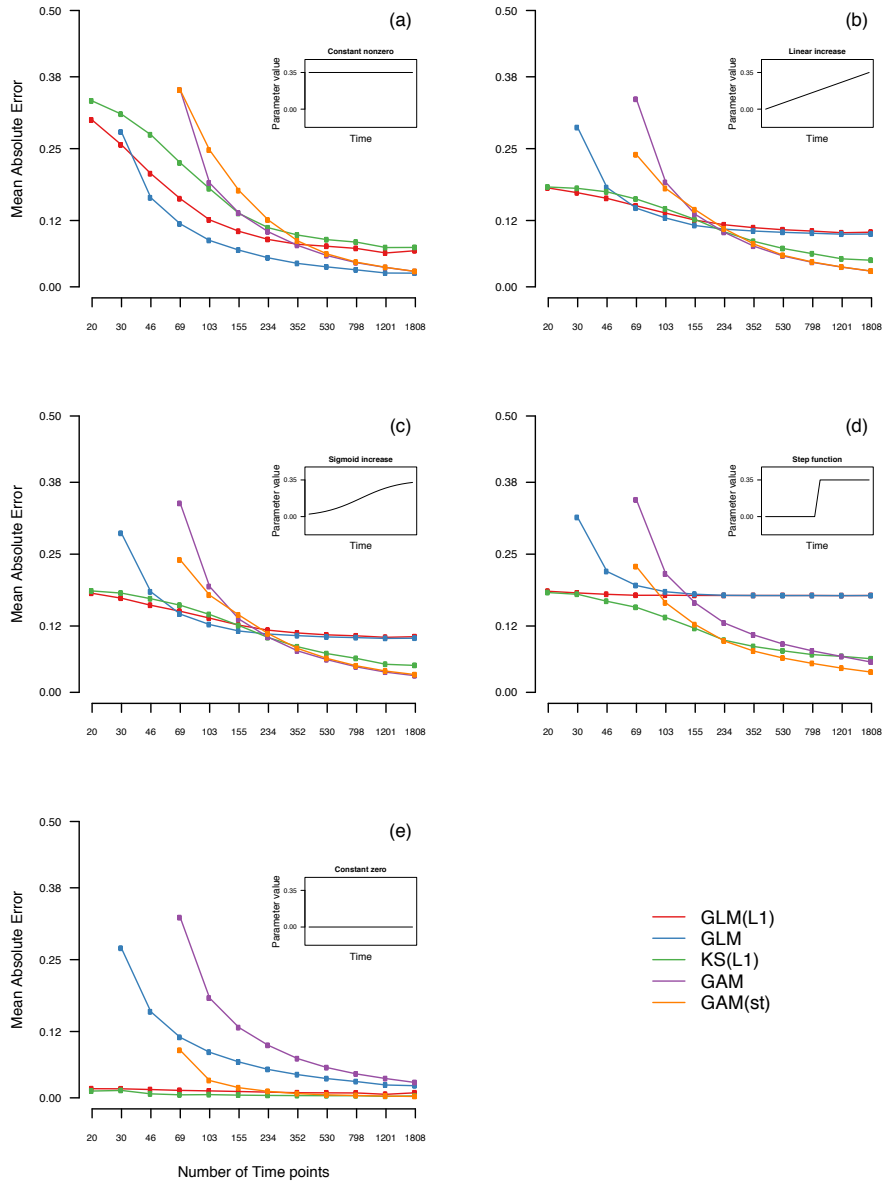


Figure 5: The five panels show the mean absolute estimation error averaged over the same type, time points, and iterations as a function of the number of observations  $n$  on a log scale. We report the error of five estimation methods: stationary  $\ell_1$ -regularized regression (red), unregularized regression (blue), time-varying  $\ell_1$ -regularized regression via kernel-smoothing (green), time-varying regression via GAM (purple), and time-varying regression via GAM with thresholding at 95% CI (orange). Some data points are missing because the respective models are not identified in that situation (see Section 3.2).

We first look at the results for the nonzero constant function in Figure 5 (a). For all estimation methods the error is large for small  $n$  and converges to zero as  $n$  increases. The GLM method has a lower estimation error than its  $\ell_1$ -regularized counterpart, GLM(L1). This is because the  $\ell_1$ -penalty biases estimates towards zero. The time-varying models perform worse than the stationary models. This makes sense: when choosing a stationary model we correctly assume that the parameters are stationary (constant across time). This constrains the space of possible parameters dramatically and thereby makes the estimation problem much simpler. In contrast, the flexibility of a time-varying model can only do harm in this situation, because any deviation from a constant function amounts to fitting noise. In different words, we provide additional information to the stationary methods in the form of the assumption that the true parameter function is constant. Because this assumption is true for the constant function, using it improves performance.

For the linearly increasing time-varying parameter in Figure 5 (b), the stationary methods outperform the GAM-based time-varying methods for small  $n$ . For large  $n$ , the time-varying GAM methods have a lower estimation error than the stationary models, because their flexibility to fit time-varying decreases estimation error more than their relative instability increases estimation error. The  $\ell_1$  regularized time-varying estimator is never worse than the stationary estimator and shows similar or slightly lower performance than the time-varying GAM models for large  $n$ . The GAM-based time-varying methods only become better than the stationary ones between  $n = 155$  and  $n = 235$  observations. The error of the time-varying methods converges to zero, while the error of the stationary methods converges to  $\frac{0.35}{2} = 0.175$ , which is the error of the constant function best fitting a linear increase from zero to  $\theta = 0.35$ . We see a similar behavior for the sigmoid increase (c), which is what we would expect since it is similar to the linear increase. For the step function (d), the difference between stationary and time-varying is more pronounced. This is because the step function is more time-varying in the sense that the best fitting constant (stationary) function has a larger average distance to the step function than to the linear increase and the sigmoid increase.

When comparing only the time-varying methods in their performance to estimate true nonzero parameters (a through d), we see that the  $\ell_1$ -regularized kernel-smoothing method outperforms the GAM methods for small  $n$ , while the GAM methods becomes slightly better for large  $n$ . The good performance of the  $\ell_1$ -regularized estimator for small  $n$  is explained by the low variance of the estimator. The slightly lower performance compared to the GAM-methods for large  $n$  is explained by the bias introduced by the regularization together with the fact that the variance of both estimators becomes small when  $n$  is large. When estimating true zero parameters (e), the  $\ell_1$ -regularized estimator always performs best.

### 3.3.2 Absolute error over time for constant and linear increasing function

To investigate the behavior of the different methods in estimating parameters across time, we look at the average (across iterations) absolute error for each estimation point (spanning the full time series) for the constant nonzero function and the linear increasing function for  $n = \{103, 530, 1803\}$  in Figure 6. Note that these results were already shown in aggregate form in Figure 5. For instance, the average (across time)

of estimates of the stationary  $\ell_1$ -regularized method in Figure 6 (a) corresponds to the single data point in Figure 5 (a) of the same at  $n = 103$ .

Figure 6 (a) shows the average parameter estimates of each methods for the constant function with  $n = 103$  observations. In line with the aggregate results in Figure 5, the stationary methods outperform the time-varying methods, and the unregularized methods outperform the regularized methods. For the linear increase with  $n = 103$  (d), we see that the time-varying methods follow the form of the true time-varying parameter. However, the standard deviation of the estimates (vertical lines) show that the estimates are very unstable. With increasing  $n$ , the estimates of all methods become more stable. For the constant function, the time-varying methods converge to the true parameter function slower than the stationary methods. In case of the linear increase, the time-varying methods converge to the true parameter function, while the stationary methods cannot (see also the discussion of the results in Figure 5 above). Again, the  $\ell_1$ -penalized methods perform worse in the two situations shown here with nonzero true parameter functions, since the penalty biases estimates towards zero. But this disadvantage turns into an advantage if the true parameter function is equal to zero, as discussed above in Section 3.3.1. Compared to the other time-varying methods, KS(L1) shows a deviation towards zero at the end of the time series. This is because the method uses less data at the end points of the time-series since the weighting functions are cut off at the end points (see Figure 2.3). Since the true parameters at the beginning of the time series are zero, having less data and therefore estimates that are biased towards zero does not translate into estimation error.

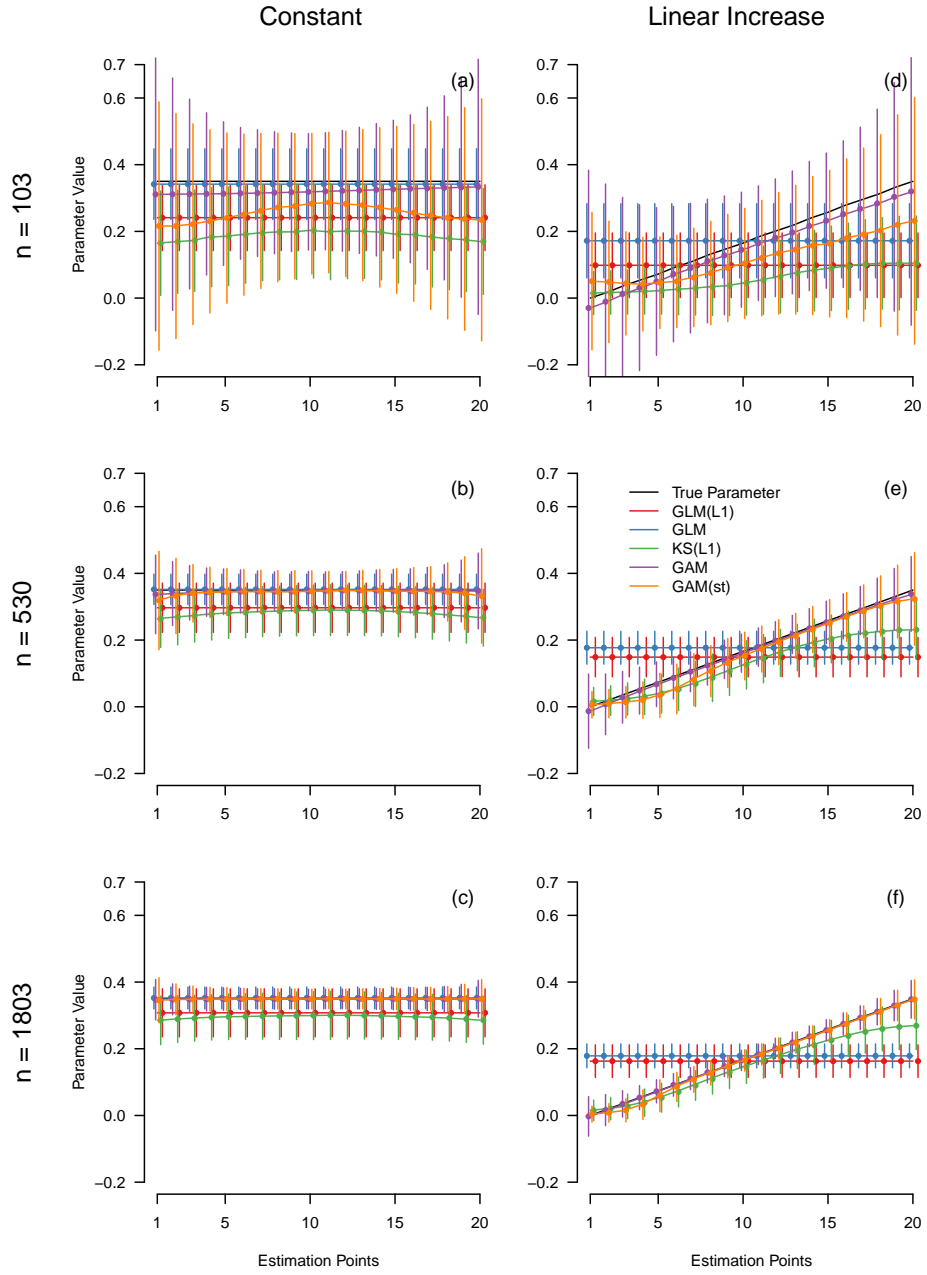


Figure 6: Mean and standard deviations of estimates for the constant parameter (left column), and the linear increasing parameter (right column), for  $n = 103$  (top row),  $n = 530$  (second row) and  $n = 1803$  (bottom row) averaged over iterations, separately for the five estimation methods: stationary  $\ell_1$ -regularized regression (red), unregularized regression (blue), time-varying  $\ell_1$ -regularized regression via kernel-smoothing (green), time-varying regression via GAM (purple), and time-varying regression via GAM with thresholding at 95% CI (orange).

### 3.3.3 Performance in structure recovery

In some situations the main interest may be to recover the *structure* of the VAR model, which is the zero-nonzero pattern in the VAR parameter matrix. We use the measures sensitivity and precision to discuss differences of the five methods in structure recovery. Sensitivity is defined as the proportion of recovered present edges,  $\frac{|\hat{E}_{\text{Present}} \cap E_{\text{Present}}|}{|\hat{E}_{\text{Present}}|}$ , where  $E = E_{\text{Present}} \cup E_{\text{Absent}}$  is the set of true edges and  $\hat{E} = \hat{E}_{\text{Present}} \cup \hat{E}_{\text{Absent}}$  is the set of edge estimates. Precision is defined as the proportion of true edges amongst the estimated edges,  $\frac{|\hat{E}_{\text{Present}} \cap E_{\text{True}}|}{|\hat{E}_{\text{Present}}|}$ . Every algorithm for structure estimation constitutes a trade-off between sensitivity and precision. Figure 7 shows this trade-off for the five estimation methods:

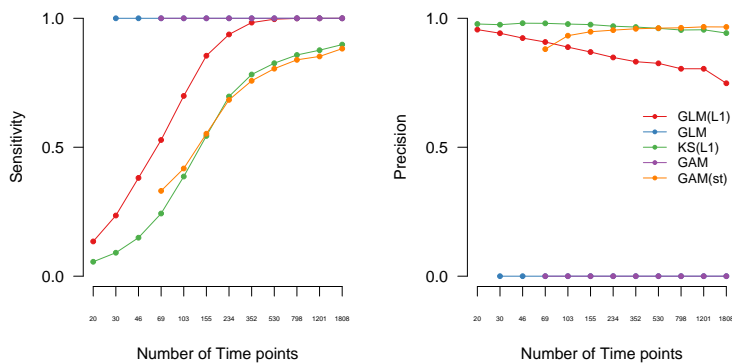


Figure 7: Sensitivity and precision for the five estimation methods across all edge-types for different variations of  $n$ . The lines for the unthresholded GAM(st) method and the stationary GAM method overlap completely, since they do not return estimates that are exactly zero. Some data points are missing because the respective models are not identified in that situation (see Section 3.2).

The unregularized stationary GLM method and the unthresholded time-varying GAM method have a sensitivity of 1 and a precision of 0 for all  $n$ . This is because these methods always return a non-zero estimate. Consequently, they estimate a nonzero value for all (true) present edges, but also a nonzero value for all (true) absent edges. It follows that these methods are inappropriate for structure estimation.

For the remaining methods, sensitivity converges to 1 as a function of  $n$ , where sensitivity converges fastest for the GLM(L1) method. The precision of GLM(L1) is lower than the precision of GAM(st) and KS(L1), since it cannot recover the absent edge in the zero half of the step function. The time-varying thresholded GAM and the kernel-smoothing method show very similar behavior, however, offer a different trade-off between sensitivity and precision (the kernel-smoothing version is slightly more liberal).



### 3.3.4 Computational Cost

Finally, in Figure 8 we depict the computational cost of the KS(L1) method versus the GAM(st) method. The computational complexity of the KS(L1) method is  $\mathcal{O}(|E|p \log p|L|)$ , where  $p$  is the number of variables,  $|E|$  is the number of estimation points and  $|L|$  is the number of lags included in the VAR model. The computational complexity for the bandwidth selection is  $\mathcal{O}(|F||Fs|p \log p|L|)$ , where  $|F|$  is the number of folds and  $|Fs|$  the number of time points in the leave-out set of each fold. For details see Haslbeck and Waldorp (2015). For the standard GAM function from the *R* package *mgcv* the computational complexity is  $\mathcal{O}(nq^2)$ , where  $n$  is the number of time points modelled, and  $q$  is the total number of coefficients, which increases if the number of basis functions increases (Wood and Augustin, 2002). Note that the credible intervals necessary for thresholding require additional computational cost. Figure 8 shows the average running time (in minutes) of the two methods for different  $p$  and  $n$  in the above reported simulation.

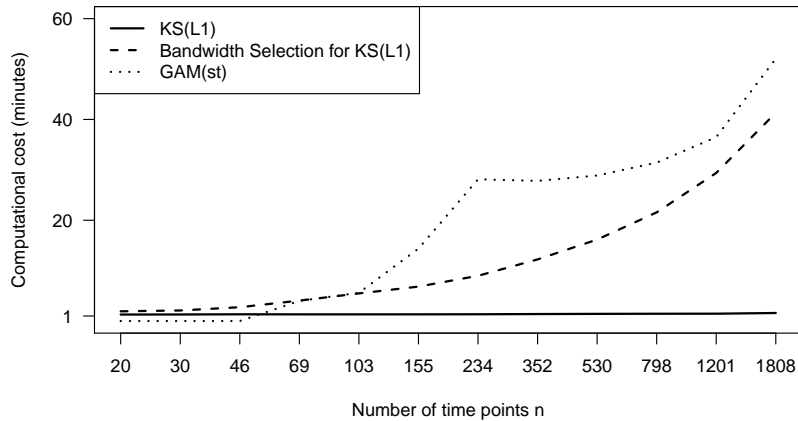


Figure 8: Computational cost in minutes to fit time-varying VAR models with the KS(L1) method (solid line) and the GAM(st) method (dotted line) as a function of observations  $n$ . The dashed line indicates the computational cost for selecting an appropriate bandwidth for the KS(L1) method.

As expected, the computational cost of KS(L1) hardly increases as a function of  $n$ . The computational cost of GAM(st) increases roughly linear as a function of  $n$ . The cost of bandwidth increases linearly as a function of  $n$ . When considering that KS(L1) requires the data-driven selection of a bandwidth parameter, the computational cost of both method is comparable for the number of variables used in our simulation. However, for larger number of variables the GAM methods become less feasible because its computational complexity quadratically depends on the number of variables. The KS(L1) method also works for huge number of variables.

### 3.4 Discussion

The KS(L1) and GAM/GAM(st) methods perform similarly but also show important differences. When  $n$  is small the estimation error of KS(L1) is much smaller.

When  $n$  is large, the estimation error of GAM/GAM(st) is slightly smaller. For true constant (stationary) parameters, KS(L1) is almost never worse than the stationary models, while GAM/GAM(st) become better than the stationary models from between  $n = 103$  and  $n = 234$ , depending on how time-varying the true parameter function is. This behavior is explained by the  $\ell_1$ -penalty used in KS(L1): the method gives relatively stable estimates (low variance), but all estimates are biased towards zero. Conversely, the GAM/GAM(st) methods use no  $\ell_1$ -penalty and hence the estimates are less stable (high variance) but are unbiased.

From the above results follows that one can always use KS(L1), even for very small  $n$ , since its performance is never worse than for the stationary models. The GAM method should be preferred if  $n$  is large and if one prefers unbiased parameter estimates. Both KS(L1) and the significance thresholded version GAM(st) set parameters to exactly zero, whereas GAM(st) is slightly more conservative. Does the fact that KS(L1) is never worse than the stationary models mean that using KS(L1) allows to detect time-varying parameters whenever they are present? No. The time-varying methods strike a balance between being stable on the one hand, and recovering the temporal dimension of parameters on the other hand. If  $n$  is large enough, the time-varying methods will recover the temporal dimension of the parameters. However, if  $n$  is small the time-varying methods trade-off the sensitivity to the temporal dimension of parameters for stability. This means that if one decreases  $n$ , the time-varying methods will allow less and less temporal variation in parameter estimates to maintain stable estimates. In other words, when decreasing  $n$ , the time-varying methods become more and more like the corresponding stationary methods.

The simulation study has three limitations: first, the signal to noise ratio  $S/N = \frac{\theta}{\sigma} = 3.5$  could be larger or smaller in a given application and the performance results would accordingly be better or worse. However, note that  $S/N$  is also a function of  $n$ . Hence if we assume a lower  $S/N$  this simply means that we need more observations to obtain the same performance, while all qualitative relationships between time-varying parameters, graph-structure and estimators remain the same.

Second, the time-varying parameters could be more time-varying. However, for estimation purposes, the extent to which a function is time-varying is determined by how much it varies over a specified time-interval *relative* to how many observations are available in that time-interval. Thus the  $n$ -variations can also be seen as a variation of "time-varying-ness": the time-varying parameter functions with  $n = 20$  vary much over time, while the parameter functions with  $n = 1808$  are hardly varying over time. Since we chose  $n$ -variations stretching from unacceptable performance ( $n = 20$ ) to very high performance ( $n = 1808$ ), we simultaneously varied the extent to which parameters are time-varying in the relevant regions.

The third limitation is that the reported performance is contingent on the particular (graph) structure we chose for the time-varying VAR model: all diagonal elements (autocorrelations) present and 35 randomly selected off-diagonal elements (cross-lagged effects) are present. This graph closely resembles a random graph, which is relatively easy to estimate. Graph structures with clusters such as small-world graphs will be harder to estimate. In fact, potentially *each* node could differ in how hard it is to estimate the parameters of the incoming effects, depending on how many there are (indegree) and how much the predicting variables are correlated. We explore the performance contingent on the indegree of a node in a second simulation

that is designed exactly for that goal. The random graph is not well suited for such an analysis for three reasons: first, sufficient data is only available for nodes with indegree close to the mean indegree (4.8) and a limited range of  $[1, 11]$ . Second, for nodes with a constant indegree the performance is different because the extent to which its predictors are correlated differs. And third, generating stable VAR models (absolute value of all eigenvalues smaller than 1) becomes increasingly hard for large  $P(\text{edge})$ . It could be that for some iterations no stable VAR models can be found in an acceptable amount of time. And we risk introducing unexpected biases through the resampling process.

In the following small simulation we avoid these problems and obtain a uniform indegree distribution with range  $[1, 20]$ . Besides allowing to investigate the performance contingent on indegree, this setup allows extrapolate the results to any graph structure to obtain a lower bound for the performance for that entire graph.

## 4 Simulation B: Upper-triangular VAR Model

The goal of this simulation is to determine the performance of all methods contingent on the indegree of a given variable in the *worst case* scenario in which all predictors are correlated with each other. Since we obtain the performance for every indegree in  $\{1, \dots, 20\}$ , the results of this simulation can be extrapolated to *any* degree distribution of a graph with  $p \leq 20$ . Specifically, one can obtain an upper bound for the error of a given time-varying parameter function for a given number of observations  $n$ .

### 4.1 Data Generation

Analogous to the first simulation, we generate time-varying VAR models in two steps: first we generate an initial graph to determine which parameters are present. In this simulation the initial graph is always the graph shown in Figure 9:

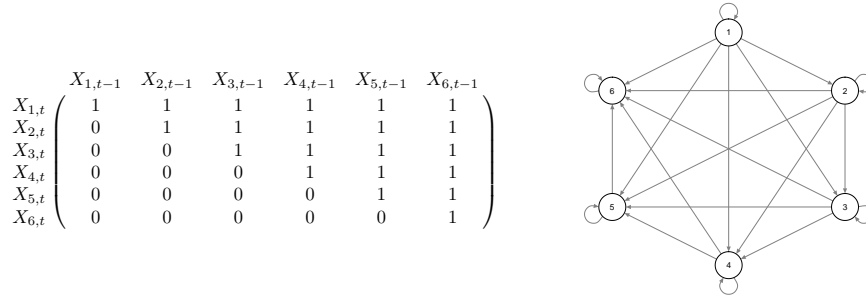


Figure 9: Left: the upper-diagonal pattern of nonzero parameters used in the time-varying VAR model in the second simulation, here shown for six variables. The row sums are equal to the indegree of the respective nodes, which results in a frequency of one for each indegree value. Right: visualization of the the upper-diagonal pattern as a directed graph. The graph used in the simulation has the same structure but is comprised of 20 nodes.

The figure visualizes a VAR parameter matrix in which all diagonal elements (autocorrelations) are nonzero and all upper-diagonal elements are nonzero. This leads to a model in which the first variable has an indegree of 1 (only autocorrelation), the second variable has an in-degree of two, and so on, and the 20th variable has an indegree of 20. In addition, this structure implies that the predictors of any variable are correlated with each other, thereby representing the worst case scenario for estimation.

In the second step we assign one of the parameter sequences (a) - (g) in Figure 4 to each nonzero parameter in the intial graph to obtain a time varying model. Similarly to the first simulation, we use the sequence of time points  $n = \{20, 30, 36, 69, 103, 155, 234, 352, 530, 798, 1201, 1808\}$ . Again, this means that each of each time-varying VAR model is parameterized by a  $p \times p \times n$  array. We set all intercepts to zero, use a maximum parameter value of  $\theta = .35$  and assign an independent Gaussian noise process with variance  $\sigma^2 = \sqrt{0.1}$  to each variable.

We estimate the model in the same way as described in Section 3.2.

## 4.2 Results

The results of the second simulation are shown in Figure 10.

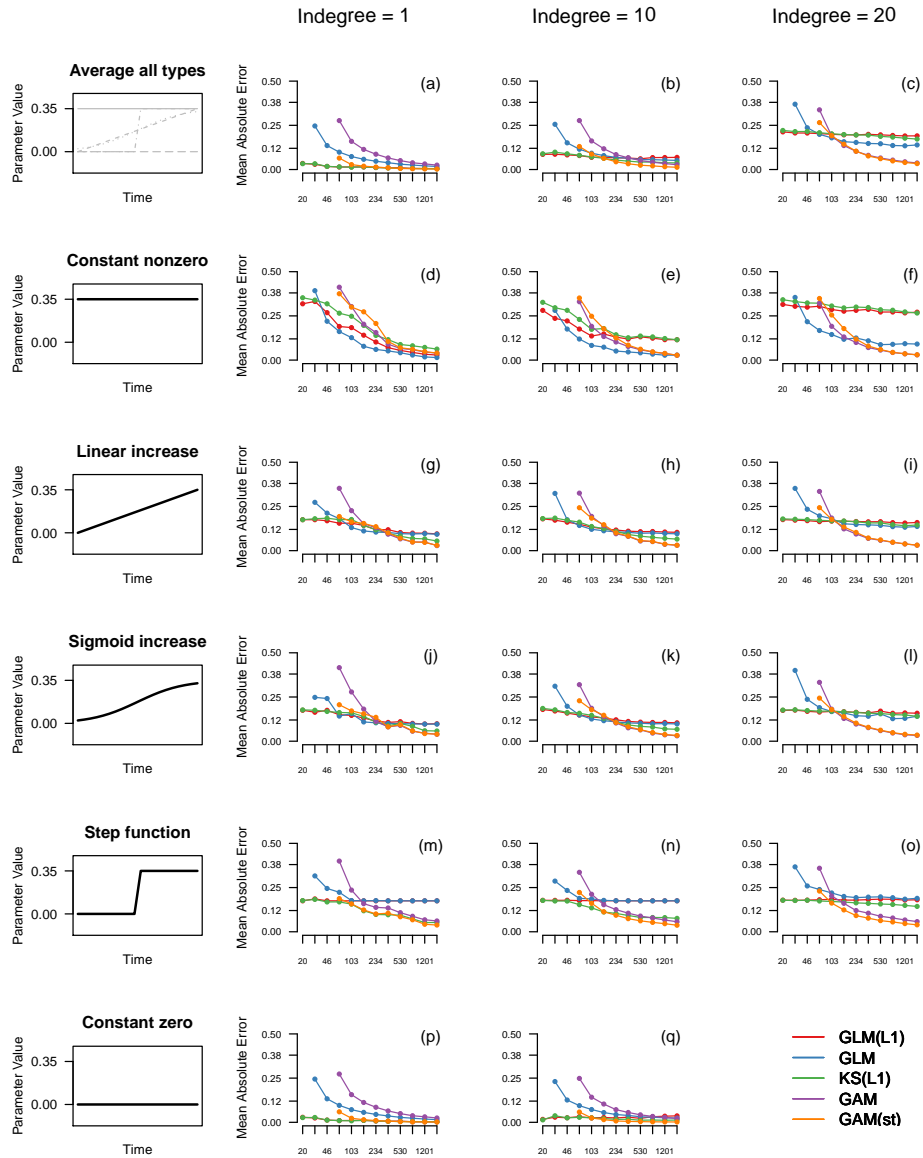


Figure 10: The mean average error for estimates of the upper-triangular model for all five estimation methods for the same sequence of numbers of time points  $n$  as in the first simulation. The results are conditioned on three different indegrees (1, 5, 20) and shown averaged across (a - c) and separately for time-varying parameter types (d - q).

The first row of Figure 3.2 shows the performance averaged over time points and types of time-varying parameters for indegree 1, 10 and 20. The first observation is

that the performance of all methods drops as a function of indegree. This is what one would expect since more parameters have to be estimated and predictors are more correlated. In addition, there is an interaction between estimation method and indegree: for indegree equal to 1 the  $\ell_1$ -penalized estimators show the *smallest* error, while for indegree equal to 20 the  $\ell_1$ -penalized estimators show the *largest* error. This is explained by the property of the  $\ell_1$ -penalized estimators, which bias all parameter estimates towards zero (see also the discussion in Section 3.3.1). This conveniently sets small parameter estimates to zero, but comes at the cost of biasing true nonzero parameter estimates towards zero. Thus, the higher the proportion of true nonzero parameters, the lower the performance of  $\ell_1$ -penalized estimators. In the case of indegree equals 20, there are no true zero parameters and hence no error is displayed (see first row in the matrix in Figure 9). This is made explicit by showing the error separately for each time-varying parameter type: for all nonzero time-varying parameters the error of  $\ell_1$ -penalized estimators increases considerably when increasing the indegree. The  $\ell_1$ -penalized estimators still outperform the other methods in setting true zero parameters to zero. However, the proportion of true-zero parameters decreases with indegree ( $\frac{10}{20} = 0.5$  for indegree 10 and  $\frac{0}{20}$  for indegree 20) which explains the drop of performance of these estimators in the average performance over types shown in the first row. All other characteristics are the same as in the random graph discussed in Section 3.

### 4.3 Discussion

The results of estimating the upper-triangular VAR model show the strengths and weaknesses of the presented methods more clearly than the random graph: if a variable has a high indegree and correlated predictors, the unbiased GAM methods show better performance. If a variable has a low indegree, which implies that most cross-lagged effects on that variable are zero, then the  $\ell_1$ -penalized methods perform better.

On the level of the full VAR model, this means that if one expects a high mean indegree, unbiased GAM methods lead to smaller estimation error. If one expects a low mean indegree and most parameters are zero,  $\ell_1$ -penalized methods will perform better. While this holds for the *average* error over the entire model, for any graph structure, the unbiased GAM methods will perform better in recovering the cross-lagged effects on a high indegree node. At the same time the  $\ell_1$ -penalized methods perform better in recovering the cross-lagged effects on a low indegree node.

In Figure 10, we showed the performance conditioned on the indegrees  $\{1, 5, 20\}$ . In the supplementary materials we provide tables with performance results of all indegrees  $\{1, 2, 3, \dots, 20\}$ . These tables allow to determine the worst-case performance in recovering the cross-lagged effects on a variable with a given indegree, with a given method and number of time points. They also allow to determine the worst-case performance of a given method and  $n$  of *any* specified graph structure, by taking the appropriate weighted average of performance results for different indegrees.

## 5 Tutorial: Application to Mood Time-Series

### 5.1 Data

We illustrate how to fit a time-varying VAR model on a symptom time series with 12 variables related to mood measured on 1476 time points during 238 consecutive days from an individual diagnosed with major depression (Wichers *et al.*, 2016). The measurements were taken at 10 pseudo-randomized time intervals with average length of 90 min between 07:30 and 22:30. During the measured time interval, a double-blind medication dose reduction was carried out, consisting of a baseline period, the dose reduction, and two post assessment periods (See Figure 11, the points on the time line correspond to the two dose reductions). For a detailed description of this data set see Kossakowski *et al.* (2017).

In the following two sections we illustrate how to estimate a time-varying VAR model using the kernel-smoothing approach (Section 5.2) and the spline-smoothing approach (Section 5.3)

### 5.2 Estimating time-varying VAR model using KS(L1)

Here we show how to estimate a time-varying VAR model using the KS(L1) method. In addition, we show how to compute time-varying prediction errors for all nodes, and how to assess the reliability of estimates. Finally, we visualize some aspects of the estimated time-varying VAR model. All analyses are performed using the R-package *mgm* (Haslbeck and Waldorp, 2015) and the shown code is fully reproducible, which means that the reader can execute the code while reading. The code below can also be found as an R-file on Github: [https://github.com/jmbh/tvvar\\_paper](https://github.com/jmbh/tvvar_paper).

#### 5.2.1 Load R-packages and dataset

The above described symptom dataset is included into the R-package *mgm* and is automatically available when loading it. After loading the package, we subset the 12 mood variables contained in this dataset:

```
library(mgm) # Version 1.2-2

mood_data <- as.matrix(symptom_data$data[, 1:12]) # Subset variables
mood_labels <- symptom_data$colnames[1:12] # Subset variable labels
colnames(mood_data) <- mood_labels
time_data <- symptom_data$data_time
```

The object `mood_data` is a  $1476 \times 12$  matrix with measurements of 12 mood variables:

```
> dim(mood_data)
[1] 1476  12

> head(mood_data[,1:7])
      Relaxed Down Irritated Satisfied Lonely Anxious Enthusiastic
[1,]      5    -1         1         5     -1     -1         4
[2,]      4     0         3         3     0      0         3
```

```

[3,]      4      0      2      3      0      0      4
[4,]      4      0      1      4      0      0      4
[5,]      4      0      2      4      0      0      4
[6,]      5      0      1      4      0      0      3

```

And `time_data` contains information about the time stamps of each measurement. This information is needed for the data preprocessing in the next section.

```

> head(time_data)
  date      dayno beepno beeptime resptime_s resptime_e  time_norm
1 13/08/12    226     1   08:58   08:58:56   09:00:15 0.000000000
2 14/08/12    227     5   14:32   14:32:09   14:33:25 0.005164874
3 14/08/12    227     6   16:17   16:17:13   16:23:16 0.005470574
4 14/08/12    227     8   18:04   18:04:10   18:06:29 0.005782097
5 14/08/12    227     9   20:57   20:58:23   21:00:18 0.006285774
6 14/08/12    227    10   21:54   21:54:15   21:56:05 0.006451726

```

### 5.2.2 Estimating time-varying VAR model

Here we describe how to use the function `tvmvar()` of the `mgm` package to estimate a time-varying VAR model. A more detailed description of this function can be found in the help file `?tvmvar`. After providing the data via the `data` argument, we specify the type and levels of each variable. The latter is necessary because `mgm` allows for different types of variables. In the present case we only have continuous variables modeled as conditional Gaussians, and we therefore specify `type = rep("g", 12)`. By convention the number of levels for continuous variables is specified as one `level = rep(1, 12)`.

Via `estpoints` we specify that we would like to have 20 estimation points that are equally spaced across the time series (for details see `?tvmvar`). Via the argument `timepoints` we provide a vector containing the time point of each measurement. The time points are used to distribute the estimation points correctly on the time interval. If no `timepoints` argument is provided, the function assumes that all measurement points are equidistant. See Section 2.5 in Haslbeck and Waldorp (2015) for a more detailed explanation how the time points are used in `mgm` and an illustration of the problems following from incorrectly assuming equidistant measurement points.

Next, we specify the bandwidth parameter  $b$ , which determines how many observations close to an estimation point are used to estimate the model at that point. Here we select  $b = 0.34$ , which we obtained by searching a candidate sequence of bandwidth parameters, and selected the value that minimized the out-of-sample prediction error in a time-stratified cross-validation scheme. The latter is implemented in the function `bwSelect()`. Since `bwSelect()` repeatedly fits time-varying VAR models with different bandwidth parameters, the specification of `bwSelect()` and the estimation function `tvmvar` are very similar. We therefore refer the reader for the code to specify `bwSelect()` to Appendix A.

After that we provide the number of the notification on a given day and the number of the day itself via the arguments `beepvar` and `dayvar`, respectively. This information is used to exclude cases from the analysis which do not have sufficient previous measurements to fit the specified VAR model. This can be both due to randomly missing data, or because of missingness by design. In the present dataset



we have both: within a given day the individual did not always answer at all 10 times. And by design, there is a break between day and night. When not considering the correct successiveness the estimated parameters do not only reflect effects from  $t_{t-1}$  on  $t$  but also effects over (possibly) many other time-lags (for instance 10h over night instead of the intended 1h30).

Via the argument `lags = 1` we specify to fit a lag 1 VAR model and choose via `lambdaSel = "CV"` to select the penalty parameter  $\lambda$  with cross-validation. Finally, with the argument `scale = TRUE` we specify that all variables should be scaled to mean zero and standard deviation 1 before the model is fit. This is recommended when using  $\ell_1$ -regularization, because otherwise the strength of the penalization of a parameter depends on the variance of the predictor variable. Since the cross-validation scheme uses random draws to define the folds, we set a seed to ensure reproducibility.

```
set.seed(1)
tvvar_obj <- tvmmvar(data = mood_data,
                    type = rep("g", 12),
                    level = rep(1, 12),
                    lambdaSel = "CV",
                    timepoints = time_data$time_norm,
                    estpoints = seq(0, nrow(mood_data) - 1, length = 20),
                    bandwidth = 0.34,
                    lags = 1,
                    beepvar = time_data$beepno,
                    dayvar = time_data$dayno,
                    scale = TRUE)
```

Before looking at the results we check how many of the 1476 time points were used for estimation, which is shown in the summary that is printed when calling the output object in the console:

```
> tvvar_obj
mgm fit-object

Model class: Time-varying mixed Vector Autoregressive (tv-mVAR) model
Lags: 1
Rows included in VAR design matrix: 876 / 1475 ( 59.39 %)
Nodes: 12
Estimation points: 20
```

This means that the VAR design matrix that is used for estimation has 876 rows. One of the removed time points is the first time point, since it does not have a previous time point. Other time points were excluded because of (a) missing measurements during the day or (b) the day-night break. As an example, from the six rows of the time stamps shown above, we could use three time points, since a measurement at the previous time point is available.

The estimated autocorrelation and cross-lagged effects are stored in the object `tvvar_obj$wadj`, which is an array of dimensions  $p \times p \times lags \times estpoints$ . For example, `tvvar_obj$wadj[1, 3, 1, 9]` returns the cross-lagged effect of variable 3 on variable 1 with the first specified lag size (here 1) at time point 9. Due to the large number of estimated parameters, we do not show this object here but instead

visualize some aspect of it in Figure 11. The signs of all parameters are stored separately in `tvvar_obj$signs`, because signs may not be defined in the presence of categorical variables (which is not the case here). The intercepts are stored in `tvvar_obj$intercepts`.

### 5.2.3 Reliability of Parameter Estimates

To judge the reliability of parameter estimates, we approximate the sampling distribution of all parameters using the nonparametric block bootstrap. The function `resample()` implements this bootstrap scheme and returns the sampling distribution and a selection of its quantiles of each parameter. First we provide the model object `object = tvvar_obj` and the data `data = mood_data`. `resample()` then fits the model specified as in `tvvar_obj` on 50 (`nB = 50`) different block bootstrap samples, where we specify the number of blocks via `blocks`. The argument `seeds` provides a random seed for each bootstrap sample and `quantiles` specifies the quantiles shown in the output.

```
res_obj <- resample(object = tvvar_obj,
  data = mood_data,
  nB = 50,
  blocks = 10,
  seeds = 1:50,
  quantiles = c(.05, .95))
```

The  $p \times p \times lags \times timepoints \times nB$  array `res_obj$bootParameters` contains the empirical sampling distribution of each parameter. For instance, the array entry `res_obj$bootParameters[1, 3, 1, 9, ]` contains the sampling distribution of the cross-lagged effect of variable 3 on variable 1 with the first specified lag size (here 1) at time point 9. Due to its size, we do not show this object here but show the 5% and 95% quantiles of the empirical sampling distribution of three time-varying parameters in Figure 11.

It is important to keep in mind that the quantiles of these bootstrapped sampling distributions are not confidence intervals around the true parameter. The reason is that the  $\ell_1$ -penalty biases all estimates and hence the whole sampling distribution towards zero which implies that the latter is not centered on the true parameter value.

### 5.2.4 Compute time-varying Prediction Error

Here we show how to compute time-varying nodewise prediction errors. Nodewise prediction errors indicate how well the model fits the data on an absolute scale and is therefore useful to judge the practical relevance of (parts of) a VAR model. See Haslbeck and Waldorp (2016) for a detailed description of nodewise prediction error (or predictability) in the context of network models and Haslbeck and Fried (2017) for an analysis of predictability in 18 datasets in the field of psychopathology.

The function `predict()` computes predictions and prediction errors from a given *mgm* model object. We first provide the model object `object = tvvar_obj` and the data `data = mood_data`. We then specify the desired types of prediction, here `R2` for the proportion of explained variance and `RMSE` for the Root Mean Squared Error. `tvMethod = "weighted"` specifies how to combine all time-varying models

to arrive at a single prediction for each variable across the whole time series (for details see `?predict`). Finally, we provide `consec = time_data$beepno` for the same reasons as above.

```
pred_obj <- predict(object = tvvar_obj,
                   data = mood_data,
                   errorCon = c("R2", "RMSE"),
                   tvMethod = "weighted",
                   consec = time_data$beepno)
```

The predictions are stored in `pred_obj$predicted` and the error of the predictions of all time-varying models combined are in `pred_obj$errors`:

```
> pred_obj$errors
  Variable Error.RMSE Error.R2
1   Relaxed    0.939   0.155
2     Down    0.825   0.297
3 Irritated    0.942   0.119
4   Satisfied    0.879   0.201
5    Lonely    0.921   0.182
6   Anxious    0.950   0.086
7 Enthusiastic    0.922   0.169
8   Suspicious    0.818   0.247
9   Cheerful    0.889   0.200
10    Guilty    0.928   0.175
11    Doubt    0.871   0.268
12   Strong    0.896   0.195
```

The prediction errors of each time-varying model separately are stored in `pred_obj$tverrors`. Note that here we weight the errors using the the same weight vector as used for estimation (see Section 2.3). For details see `?predict.mgm`. In the following section we visualize the time-varying nodewise estimation error for a subset of estimation points.

### 5.2.5 Visualize time-varying VAR model

Figure 11 visualizes a part of the time-varying VAR parameters estimated above. The top row shows visualizations of the VAR parameters for the estimation points 8, 15 and 18. Green edges indicate positive linear relationships, red edges indicate negative linear relationships. The width of the arrows is proportional to the absolute value of the corresponding parameter. The grey part of the ring around each node indicates the proportion of explained variance of each variables by all other variables in the model.

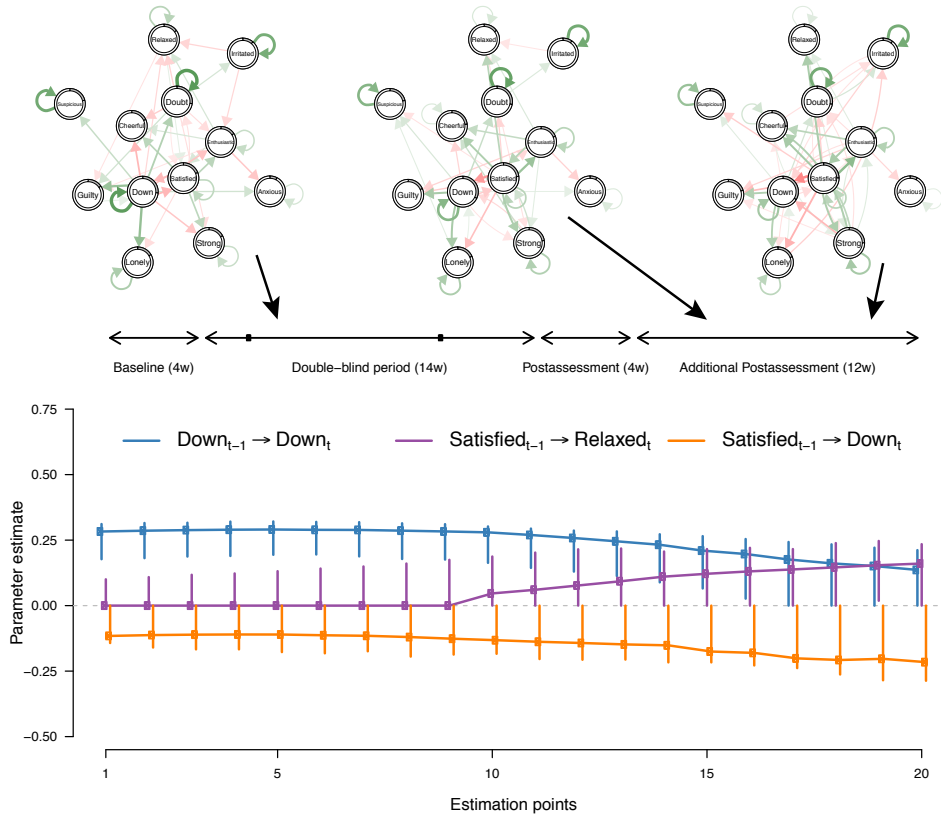


Figure 11: Top row: visualization of lag 1 VAR models at estimation points 8, 15 and 18, estimated with the KS(L1) method. Green arrows indicate positive relationships, red arrows indicate negative relationships, and the width of the arrows is proportional to the absolute value of the corresponding parameter. The self-loops indicate autocorrelations. Bottom row: three parameters plotted as a function of time; the points are the point estimate obtained from the full dataset, the vertical lines indicate the 5% and 95% quantiles of the bootstrapped sampling distribution at each estimation point.

The bottom row shows the time-varying parameters of the autoregressive effect  $\text{Down}_{t-1} \rightarrow \text{Down}_t$  and the cross-lagged effects  $\text{Satisfied}_{t-1} \rightarrow \text{Relaxed}_t$  and  $\text{Satisfied}_{t-1} \rightarrow \text{Down}_t$ . The vertical lines indicate the 5% and 95% quantiles of the empirical sampling distribution obtained from `resample()`. The code to fully reproduce Figure 11 is not shown here due to its length, but can be obtained from Github [https://github.com/jmbh/tvvar\\_paper](https://github.com/jmbh/tvvar_paper).

### 5.3 Estimating time-varying VAR model via GAM(st)

Here we show how to estimate a time-varying VAR model via the GAM(st) method. All analyses are performed using the R-package *tvvarGAM* (Bringmann and Haslbeck,

2017) and the shown code is fully reproducible, which means that the reader can execute the code while reading. The code below can also be found in an R-file on Github: [https://github.com/jmbh/tvvar\\_paper](https://github.com/jmbh/tvvar_paper).

### 5.3.1 Load R-packages and dataset

Similarly to Section 5.2.1 we load the dataset from the *mgm* package, and subset the 12 mood related variables. In addition, we load the *tvvarGAM* package.

```
library(mgm) # Version 1.2-2

mood_data <- as.matrix(symptom_data$data[, 1:12]) # Subset variables
mood_labels <- symptom_data$colnames[1:12] # Subset variable labels
colnames(mood_data) <- mood_labels
time_data <- symptom_data$data_time

# For now from github:
library(devtools)
install_github("LauraBringmann/tvvarGAM")
library(tvvarGAM)
```

### 5.3.2 Estimating time-varying VAR model

We use the function `tvvarGAM()` to estimate the time-varying VAR model. We provide the data via the `data` argument and provide an integer vector of length  $n$  indicating the successiveness of measurements by specifying the number of the recorded notification and the day number via the arguments `beepvar` and `dayvar`. The latter is used similarly as in the *mgm* package to compute the VAR design matrix. Via the argument `nb` we specify the number of desired basis functions (see Section 2.2). First, we estimated the model with 10 basis functions. However, because some of the edf of the smooth terms were close to 10, we doubled the number of basis functions (see discussion in Section 2.2).

```
tvvargam_obj <- tvvarGAM(data = mood_data,
                        nb = 20,
                        beepvar = time_data$beepno,
                        dayvar = time_data$dayno,
                        estimates = TRUE,
                        plot = FALSE)
```

The output object consists of a list with three entries:

`tvvargam_obj$Results_GAM$Estimate` is a  $(p + 1) \times p \times \text{timepoints}$  array that contains the parameter estimate at each time point. The first row contains the estimated intercepts. The two other list entries have the same dimensions and contain the 5% and 95% confidence intervals for the estimates in `tvvargam_obj$Results_GAM$Estimate`. Thus, in case of the *tvvarGAM* package no separate resampling scheme is necessary in order to get a measure for the reliability of parameters.

### 5.3.3 Visualize time-varying VAR model

Figure 12 visualizes the part of the time-varying VAR like Figure 11 above, however, now with the estimates from the *tvarGAM* package. Notice that for visualization purposes we used the thresholded version of the time-varying VAR, thus showing only the arrows that are significant ( $p$ -value  $< 0.05$ ).

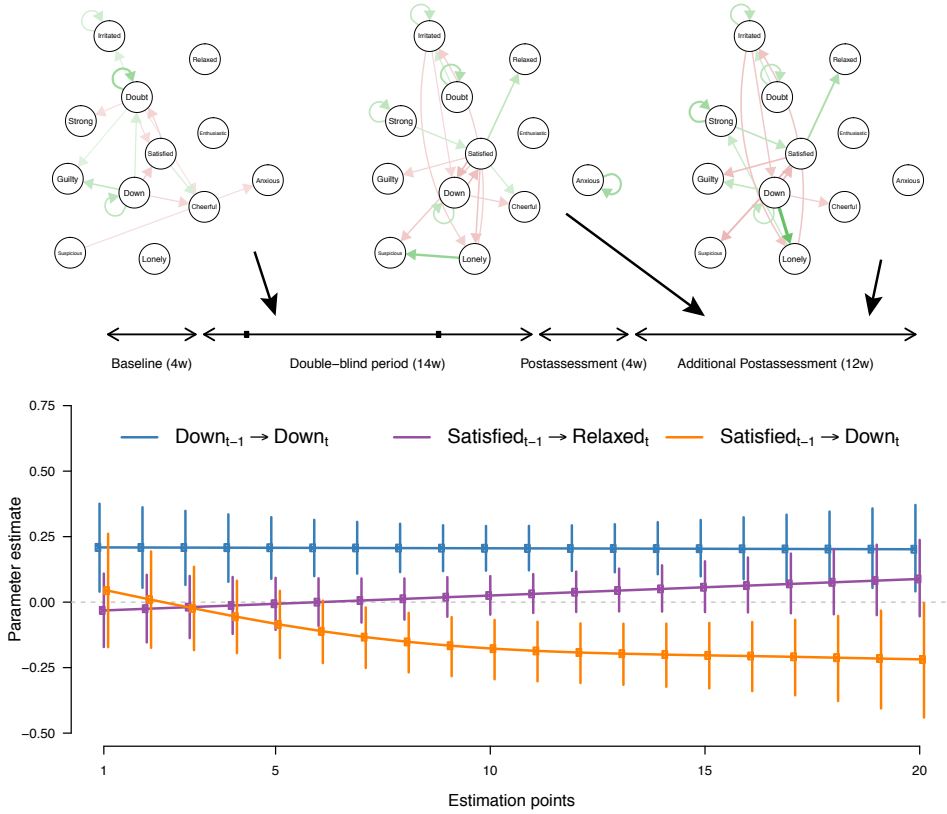


Figure 12: Top row: visualization of thresholded VAR models at estimation points 8, 15 and 18, estimated with the spline-based method. Green arrows indicate positive relationships, red arrows indicate negative relationships, and the width of the arrows is proportional to the absolute value of the corresponding parameter. The self-loops indicate autocorrelations. Bottom row: three parameters plotted as a function of time; the points are unthresholded point estimates, the vertical lines indicate the 5% and 95% credible intervals at each estimation point.

As to be expected from the similar performance of the two methods in our simulations, the results look similar. The code to fully reproduce Figure 12 is not shown here due to its length, but can be obtained from Github [https://github.com/jmbh/tvvar\\_paper](https://github.com/jmbh/tvvar_paper).

## 6 Conclusions

We presented two methods to estimate time-varying VAR models: one is based on spline-smoothing (GAM/GAM(st)) and the other is based on penalized kernel-smoothing (KS(L1)). We compared the performance of these two methods and their stationary counter-parts in situations that are typically encountered in practice. Our simulation results allow researchers to plan studies with sufficient observations to detect the phenomena of interest and to judge the stability of VAR estimates in a given (time-varying) VAR model. In addition, we provided fully reproducible code examples showing how to estimate time-varying VAR models with both methods, using free and open source R-packages.

It would also be interesting to investigate the performance of both methods for mixed VAR models, where different variables are associated with exponential family distributions other than Gaussians, for instance Bernoulli, multinomial, exponential or Poisson. These time-varying mixed VAR models can be estimated with the *mgm* package (Haslbeck and Waldorp, 2015). However, we did not study the performance of recovering time-varying mixed VAR models using the kernel-smoothing method, because our main goal in this paper was to compare the kernel-smoothing method with the spline-smoothing method, which is only implemented for VAR models with Gaussian noise. A model related to the VAR model is the graphical VAR model (Abegaz and Wit, 2013), which estimates both the VAR parameters and the residual structure  $\Sigma$  (see Section 2.1). In this model, identifying time-varying parameters is especially important, because spurious relations in the residual structure can be induced by time-varying parameters. We leave this for future work.

## Acknowledgements

We would like to thank Denny Borsboom, Marie Deserno, Oisín Ryan and Sacha Epskamp for their useful comments on earlier versions of this manuscript. We would like to thank Simon Wood explaining several details about his R-package *mgcv*. This research was supported by European Research Council Consolidator Grant no. 647209.

## References

- aan het Rot, M., Hogenelst, K., and Schoevers, R. A. (2012). Mood disorders in everyday life: A systematic review of experience sampling and ecological momentary assessment studies. *Clinical psychology review*, **32**(6), 510–523.
- Abegaz, F. and Wit, E. (2013). Sparse time series chain graphical models for reconstructing genetic networks. *Biostatistics*, **14**(3), 586–599.
- Andersen, R. (2009). Nonparametric methods for modeling nonlinearity in regression analysis. *Annual Review of Sociology*, **35**, 67–85.
- Bak, M., Drukker, M., Hasmi, L., and van Os, J. (2016). An n= 1 clinical network analysis of symptoms and treatment in psychosis. *PloS one*, **11**(9), e0162811.

- Belsley, D. A. and Kuti, E. (1973). Time-varying parameter structures: An overview. In *Annals of Economic and Social Measurement, Volume 2, number 4*, pages 375–379. NBER.
- Bringmann, L. F. and Haslbeck, J. M. B. (2017). tvvargam. <https://github.com/LauraBringmann/tvvarGAM>.
- Bringmann, L. F., Vissers, N., Wichers, M., Geschwind, N., Kuppens, P., Peeters, F., Borsboom, D., and Tuerlinckx, F. (2013). A network approach to psychopathology: new insights into clinical longitudinal data. *PLoS one*, **8**(4), e60188.
- Bringmann, L. F., Ferrer, E., Hamaker, E., Borsboom, D., and Tuerlinckx, F. (2015). Modeling nonstationary emotion dynamics in dyads using a semiparametric time-varying vector autoregressive model.
- Bringmann, L. F., Hamaker, E. L., Vigo, D. E., Aubert, A., Borsboom, D., and Tuerlinckx, F. (2017). Changing dynamics: Time-varying autoregressive models using generalized additive modeling. *Psychological Methods*.
- Dakos, V. and Lahti, L. (2013). R early warning signals toolbox. *The R Project for Statistical Computing*. <http://cran.r-project.org/web/packages/earlywarnings/index.html>.
- Epskamp, S., Waldorp, L. J., Möttus, R., and Borsboom, D. (2016). Discovering psychological dynamics: The gaussian graphical model in cross-sectional and time-series data. *arXiv preprint arXiv:1609.04156*.
- Friedman, J., Hastie, T., and Tibshirani, R. (2010). Regularization paths for generalized linear models via coordinate descent. *Journal of statistical software*, **33**(1), 1.
- Gibberd, A. J. and Nelson, J. D. (2017). Regularized estimation of piecewise constant gaussian graphical models: The group-fused graphical lasso. *Journal of Computational and Graphical Statistics*, (just-accepted).
- Gibbert, A. (2017). Graphtime. <https://github.com/GlooperLabs/GraphTime>.
- Golub, G. H., Heath, M., and Wahba, G. (1979). Generalized cross-validation as a method for choosing a good ridge parameter. *Technometrics*, **21**(2), 215–223.
- Hamilton, J. D. (1994). *Time series analysis*, volume 2. Princeton university press Princeton.
- Hartmann, J. A., Wichers, M., Menne-Lothmann, C., Kramer, I., Viechtbauer, W., Peeters, F., Schruers, K. R., van Bemmelen, A. L., Myin-Germeys, I., Delespaul, P., *et al.* (2015). Experience sampling-based personalized feedback and positive affect: a randomized controlled trial in depressed patients. *PLoS One*, **10**(6), e0128095.
- Haslbeck, J. M. B. and Fried, E. I. (2017). How predictable are symptoms in psychopathological networks? a reanalysis of 18 published datasets. *Psychological Medicine*, pages 1–10.



- Haslbeck, J. M. B. and Waldorp, L. J. (2015). mgm: Structure estimation for time-varying mixed graphical models in high-dimensional data. *arXiv preprint arXiv:1510.06871*.
- Haslbeck, J. M. B. and Waldorp, L. J. (2016). How well do network models predict future observations? on the importance of predictability in network models. *arXiv preprint arXiv:1610.09108*.
- Hastie, T., Tibshirani, R., and Wainwright, M. (2015). *Statistical learning with sparsity*. CRC press.
- Holmes, E., Ward, E., and Wills, K. (2013). *MARSS: Multivariate Autoregressive State-Space Modeling*. R package version 3.9.
- Holmes, E. E., Ward, E. J., and Wills, K. (2012). Marss: Multivariate autoregressive state-space models for analyzing time-series data. *The R Journal*, **4**(1), 30.
- Keele, L. J. (2008). *Semiparametric regression for the social sciences*. Chichester, England: John Wiley & Sons.
- Kossakowski, J., Groot, P., Haslbeck, J. M. B., Borsboom, D., and Wichers, M. (2017). Data from critical slowing down as a personalized early warning signal for depression. *Journal of Open Psychology Data*, **5**(1).
- Kramer, I., Simons, C. J., Hartmann, J. A., Menne-Lothmann, C., Viechtbauer, W., Peeters, F., Schruers, K., Bemmél, A. L., Myin-Germeys, I., Delespaul, P., *et al.* (2014). A therapeutic application of the experience sampling method in the treatment of depression: a randomized controlled trial. *World Psychiatry*, **13**(1), 68–77.
- Kroeze, R., Van Veen, D., Servaas, M. N., Bastiaansen, J. A., Oude Voshaar, R., Borsboom, D., and Riese, H. (2016). Personalized feedback on symptom dynamics of psychopathology: a proof-of-principle study. *J Person-Orient Res*.
- Monti, R. (2014). pysingle. <https://github.com/piomonti/pySINGLE>.
- Monti, R. P., Hellyer, P., Sharp, D., Leech, R., Anagnostopoulos, C., and Montana, G. (2014). Estimating time-varying brain connectivity networks from functional MRI time series. *Neuroimage*, **103**, 427–443.
- Shadish, W. R., Zuur, A. F., and Sullivan, K. J. (2014). Using generalized additive (mixed) models to analyze single case designs. *Journal of School Psychology*, **52**(2), 149–178.
- Snippe, E., Viechtbauer, W., Geschwind, N., Klippel, A., De Jonge, P., and Wichers, M. (2017). The impact of treatments for depression on the dynamic network structure of mental states: Two randomized controlled trials. *Scientific Reports*, **7**.
- Tarvainen, M. P., Hiltunen, J. K., Ranta-aho, P. O., and Karjalainen, P. A. (2004). Estimation of nonstationary eeg with kalman smoother approach: an application to event-related synchronization (ers). *IEEE Transactions on Biomedical Engineering*, **51**(3), 516–524.

- van der Krieke, L., Blaauw, F. J., Emerencia, A. C., Schenk, H. M., Slaets, J. P., Bos, E. H., de Jonge, P., and Jeronimus, B. F. (2017). Temporal dynamics of health and well-being: A crowdsourcing approach to momentary assessments and automated generation of personalized feedback. *Psychosomatic medicine*, **79**(2), 213–223.
- Wichers, M., Groot, P. C., Psychosystems, E., Group, E., *et al.* (2016). Critical slowing down as a personalized early warning signal for depression. *Psychotherapy and psychosomatics*, **85**(2), 114–116.
- Wigman, J., van Os, J., Borsboom, D., Wardenaar, K., Epskamp, S., Klippel, A., Viechtbauer, W., Myin-Germeys, I., and Wichers, M. (2015). Exploring the underlying structure of mental disorders: cross-diagnostic differences and similarities from a network perspective using both a top-down and a bottom-up approach. *Psychological medicine*, **45**(11), 2375–2387.
- Wood, S. N. (2006). *Generalized additive models: An introduction with R*. Boca Raton, FL: Chapman and Hall/CRC.
- Wood, S. N. and Augustin, N. H. (2002). Gams with integrated model selection using penalized regression splines and applications to environmental modelling. *Ecological modelling*, **157**(2), 157–177.

## A Code to select appropriate bandwidth in KS(L1) method

The function `bwSelect()` fits time-varying VAR models with different bandwidth parameters to a set of training sets and computes the out-of-sample prediction error in the hold-out sets. We then select the bandwidth that minimizes this prediction error across variables and hold-out sets. For details about how these training/test sets are chosen exactly see `?bwSelect` or Haslbeck and Waldorp (2015).

Since we fit the time-varying VAR model of our choice repeatedly, we provide all parameters we specified to the estimation function `tvmvar()` as described in Section 5.2.2. In addition, we specify via `bwFolds` the number of training set / test set splits, via `bwFoldsize` the size of the test sets, and via `bwSeq` the sequence of candidate bandwidth-values. Here, we chose ten equally spaced values in  $[0.01, 1]$ .

```
bwSeq <- seq(0.01, 1, length = 10)

bw_object <- bwSelect(data = mood_data,
                     type = rep("g", 12),
                     level = rep(1, 12),
                     bwSeq = bwSeq,
                     bwFolds = 1,
                     bwFoldsize = 20,
                     modeltype = "mvar",
                     lags = 1,
                     scale = TRUE,
                     timepoints = time_data$time_norm,
```

```

beepvar = time_data$beepno,
dayvar = time_data$dayno,
pbar = TRUE)

bandwidth <- bwSeq[which.min(bw_object$meanError)]

[1] 0.34

```

The output object `bw_object` contains all fitted models and unaggregated prediction errors. We see that the bandwidth 0.34 minimized the average out-of-sample prediction error. The full bandwidth path is shown in Figure 13.

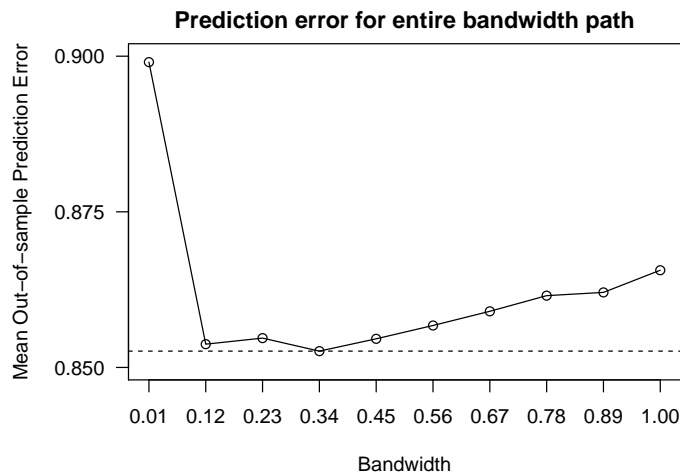


Figure 13: Average out-of-sample prediction error for different bandwidth values obtained from the function. The bandwidth value 0.34 returns the smallest error, indicated by the dashed line.

The bandwidth value of 0.1 is clearly too small, indicated by a large prediction error. The error then tends to become smaller as a function of  $b$  until its minimum at 0.34 and then increases again. Note that if the smallest/largest considered bandwidth value minimizes the error, another search should be conducted with smaller/larger bandwidth values.